3 Thoracolumbar Spinal Arterial Anatomy, with Special Consideration Given to Spine Intervention

Philippe Gailloud

Introduction

This chapter reviews the basic concepts governing the organization of the spinal cord supply and describes spinal arterial features relevant to the safe conduct of endovascular and percutaneous spine procedures.

Spinal Arterial System

The Intersegmental Artery

A discussion of the arterial vascularization of the spine and spinal cord primarily consists in a description of the intersegmental artery (ISA). Primitive ISAs are posterior branches of the embryonic dorsal aortas; their ostia remain separate after the formation of a single adult aorta, except in the lower lumbar region, where paired ISAs sharing a common stem are common (i.e., bilateral intersegmental trunks). Thoracic bilateral trunks are exceptional and generally multiple [1].

Thoracic and lumbar ISAs remain close to their primitive configuration, which includes an aortic stem and three branches (i.e., spinal, dorsal, and lateral) (Fig. 3.1). Cervical and sacral ISAs undergo secondary modifications to form the vertebral and lateral sacral arteries (Figs. 3.2 and 3.3) [2, 3].

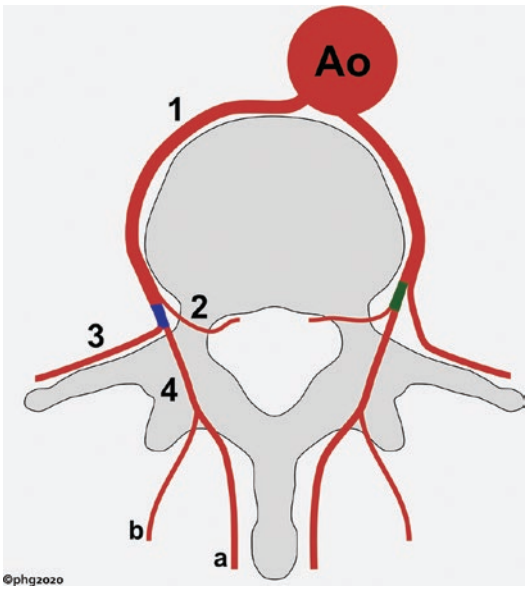

Fig. 3.1 Basic anatomy of the intersegmental artery. Ao = aorta, 1 = aortic stem, 2 = spinal (or medial) branch, 3 = lateral branch, 4 = dorsal branch, with medial, **a**, and lateral, **b**, muscular arteries. A proximal origin of the lateral branch results in the formation of a short trunk for the medial and dorsal branches (*left side*, *green segment*), i.e., the so-called dorsospinal artery. A dorsolateral artery is not present when the lateral branch takes off more distally; instead, a common segment for the lateral and dorsal branches is formed (right side, blue segment). The three branches occasionally trifurcate. (© 2021 Philippe H. Gailloud. All Rights Reserved)

P. Gailloud (✉)
Division of Interventional Neuroradiology,
Department of Radiology and Radiological Science,
The Johns Hopkins Hospital, Baltimore, MD, USA

M. Khan et al. (eds.), *Image Guided Interventions of the Spine*,
https://doi.org/10.1007/978-3-030-80079-6_3

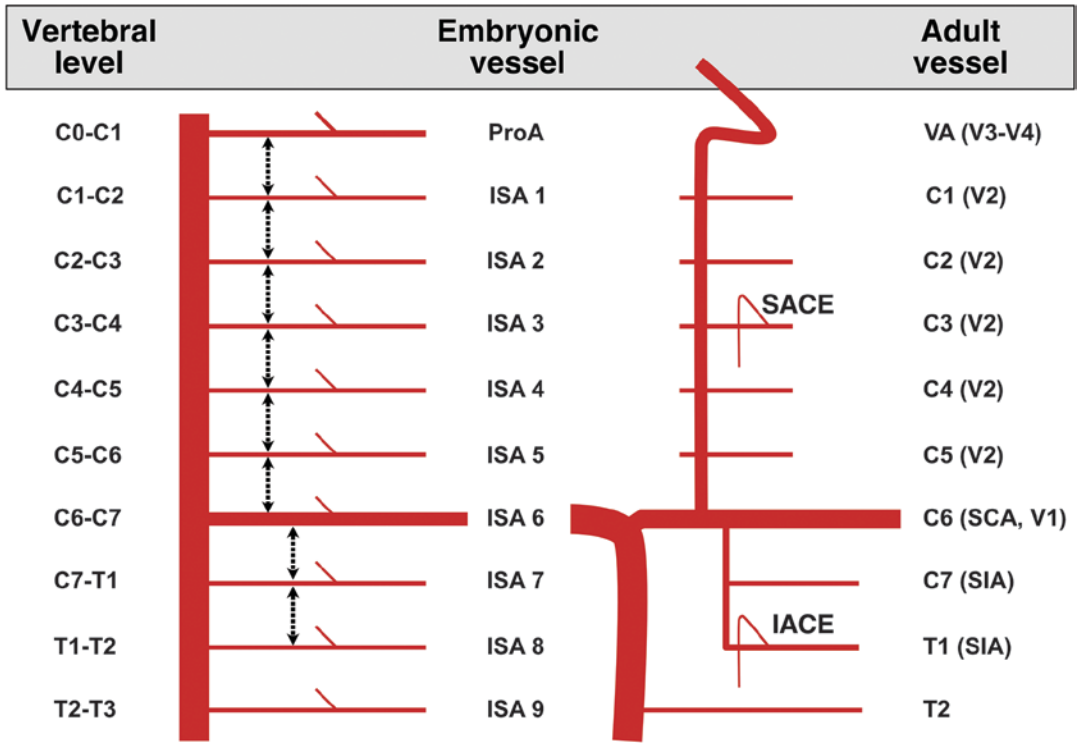

Fig. 3.2 Modifications of the intersegmental pattern at the cervical level. The intersegmental artery (ISA) coursing along the first cervical nerve, between the occiput and the first cervical vertebra (C0–C1), is the proatlantal artery (ProA), which forms part of the distal adult vertebral artery (VA, segments V3 and V4). The subclavian artery (SCA) derives from the 6th cervical ISA (ISA 6) at the C6–C7 level. A series of anastomotic connections established between the ProA and the SCA forms part of the adult VA (V2 segment). The origin of the VA (V1 segment) is made of a persistent cervical or thoracic ISA, generally the 6th cervical ISA. The persistent ISA forming the V1 segment can be determined by its point of entrance into the transverse canal: for example, the VA normally passes through a C6 transverse foramen, while a persistent 5th cervical ISA crosses a C5 transverse foramen. The persistence of more than one primitive ISA results in the formation of a VA duplication or—exceptionally—triplication [2]. The supreme intercostal artery (SIA) is made of pretransverse anastomoses linking the 7th cervical ISA (ISA 7) to the first and—less commonly—second thoracic ISAs (ISAs 8 and 9). The SIA may occasionally include the 3rd thoracic ISA (ISA 10); in its most limited form, it only consists of the 7th cervical ISA [3]. The superior and inferior arteries of the cervical enlargement are represented at C3 (sace) and T1 (iace), respectively. (© 2021 Philippe H. Gailloud. All Rights Reserved)

A unilateral intersegmental trunk is a single aortic stem branching off two or more ipsilateral ISAs; the supreme intercostal artery is a near constant example of unilateral trunk (Fig. 3.4) [4]. A complete unilateral trunk provides a full set of intersegmental branches (i.e., spinal, lateral, and dorsal) for each vertebral level involved. An incomplete trunk is an angiographic pitfall since the missing branches typically arise from the aorta as a separate vessel—an isolated dorsospinal artery [5]—that often provides a prominent radiculomedullary artery (RMA) [6] (Fig. 3.5).

Muscular Branches

Paraspinal Musculature The dorsal branch of the ISA supplies the paraspinal musculature via medial, intermediate, and lateral muscular rami. Posterior perforating branches of the posterior intercostal and lumbar arteries also contribute to the muscular vascularization, either directly or by anastomosing with the lateral rami of dorsal

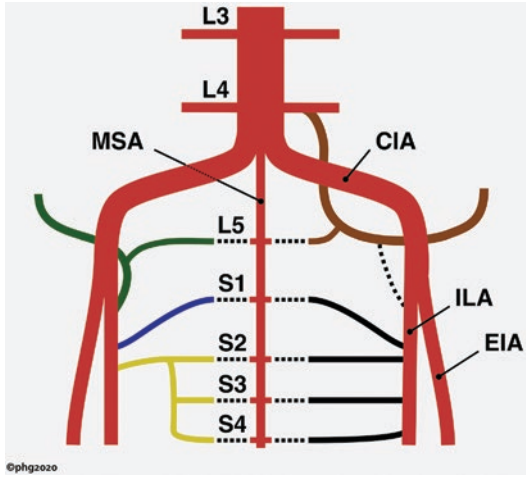

Fig. 3.3 Modifications of the intersegmental pattern at the sacral level. The anatomy of the intersegmental arteries (ISA) proximal to the takeoff of the common iliac arteries (CIA) remains unchanged (e.g., L3 and L4). The aorta continues beyond the aortoiliac bifurcation as the median sacral artery (MSA), which keeps a typical aortic morphology, notably sending paired intersegmental sacral contributions. Depending on the level of the aortoiliac bifurcation, the MSA branches off both the 4th and 5th lumbar ISAs or just the latter, as depicted in this illustration. The respective contributions of branches of aortic and iliac origins vary at the adult stage. In general, L5 is supplied by the lumbar branch of the iliolumbar artery (right side, green vessel), with additional contributions from the MSA and the L4 ISA. The most common branching pattern of the lateral sacral arteries involves two trunks, the superior (*right side, blue vessel*, S1) and inferior (*yellow vessel*, S2, S3, and S4) lateral sacral arteries. Other configurations are possible, such as a separate origin of each sacral ISA from the internal iliac artery (ILA), as depicted on the left side. The lumbosacral anastomotic circle centered on L5 is prone to variations: for example, the iliolumbar and L5 vertebral territories can be supplied by a dominant L4 anastomosis (*left side, brown vessel*). EIA = external iliac artery. (© 2021 Philippe H. Gailloud. All Rights Reserved)

branches (Fig. 3.6). Muscular branches from opposite and adjacent ISAs form an intricate paraspinal network, which often takes part in the development of collateral pathways, for example, in patients with aortic atheroma, but also represents a pitfall during embolotherapy ("dangerous anastomoses").

Upper thoracic muscular branches have a typical course including a short ascending segment, a sharp downward curve, and a long descending segment; they can mimic a bronchial artery, an RMA, or even the draining vein of an arteriovenous fistula (Fig. 3.7). The occlusion of muscular branches during embolotherapy is usually not a concern, but instances of paraspinal muscle infarction—likely in a context of widespread occlusion—have been reported [7].

Psoas Arteries At the lumbar level, the lateral (or abdominal wall) branches of the ISA pass in between the psoas muscle and the lumbar plexus, providing neural branches that course downward along each lumbar nerve [8]. Anterolateral muscular branches are usually small, but the arteries supplying the psoas muscles represent a notable exception: lumbar intersegmental stems provide conspicuous superficial and deep branches easily identified by their oblique course aligned with the psoas fibers [9] (see Fig. 3.6).

Implication for Spine Intervention

The aortic stem of thoracic and lumbar ISAs, tightly wrapped around the vertebral body wall, can be injured during open [10] or percutaneous [11] spine interventions (Fig. 3.8). Besides spinal cord ischemia and immediate hemorrhage, ISA stem injuries can lead to the formation of pseudoaneurysms with potentially severe, delayed, and occasionally fatal complications [12] (*Illustrative case 1*). Spine procedures often damage distal muscular rami [13], but these injuries rarely cause major hemorrhages.

Passage of bone cement into an ISA during vertebral augmentation procedures is rare but potentially dramatic when distal migration into spinal [14] or peripheral [15] arteries occurs. Untoward ISA embolization is more likely to happen with hypervascular lesions [16]. The mechanism may involve direct puncture of an ISA or one of its branches or, in lesions with arteriovenous shunting, retrograde arterial passage of the embolic agent, possibly after occlusion of the venous side of the shunt (Fig. 3.9). Extrinsic ISA compression by leaking bone cement can also lead to neurological complications (*Illustrative case 2*).

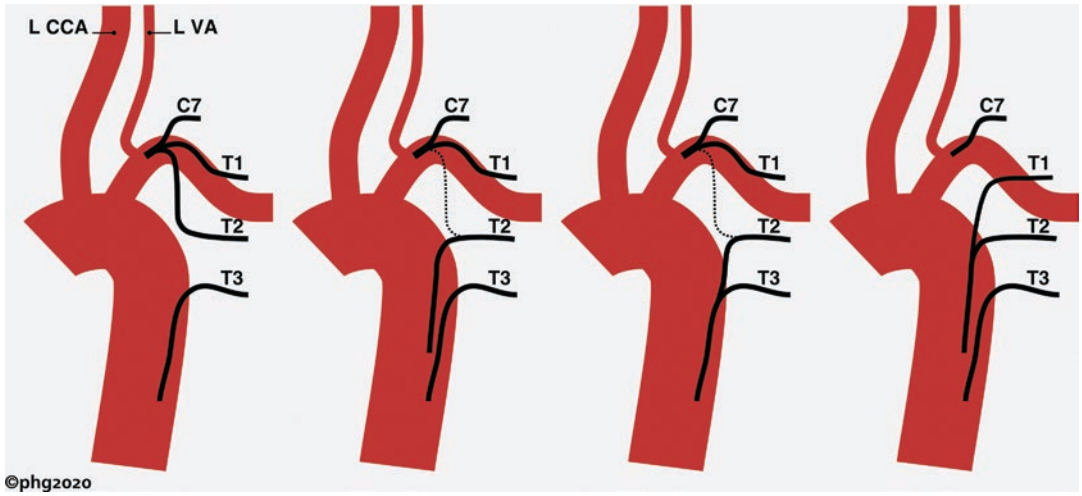

Fig. 3.4 The supreme intercostal artery and the cervicothoracic junction. Variations in the configuration of the supreme intercostal artery (SIA) and the origin of the superior thoracic intersegmental arteries (ISAs) influence the number of ISAs studied during the aortic phase of a spinal angiogram. L CCA = left common carotid artery, L VA = left vertebral artery. *Left to right:* "Textbook" configuration, in which the SIA provides the C7, T1, and T2 ISAs, while the T3 ISA comes from the thoracic aorta. Common variant, in which the second thoracic ISA (T2) has a separate aortic origin, generally with minor residual anastomotic connections (*dotted line*). Common variant, in which the second thoracic ISA (T2) has a shared aortic origin with the third thoracic ISA (T3) (i.e., unilateral T2–T3 intersegmental trunk). Rare variant, in which the SIA is only formed by the last cervical ISA (C7); in that case, the first thoracic ISA (T1) typically shares its origin with T2 or with a T2–T3 trunk.

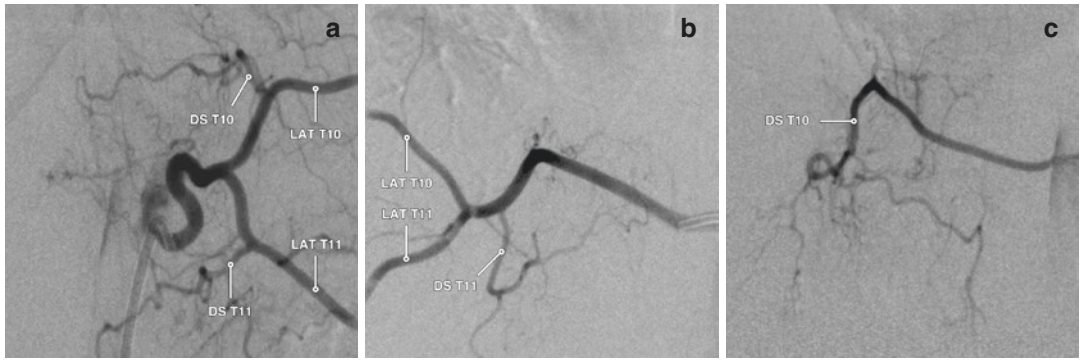

Fig. 3.5 Complete and incomplete unilateral intersegmental trunks. (**a**) Digital subtraction angiography (DSA), left T10–T11 complete unilateral intersegmental trunk injection, PA view. Each level has lateral branch (LAT) and a dorsospinal artery (DS). (**b**) DSA, right T10–T11 incomplete unilateral intersegmental trunk injection, PA view. The dorsospinal component is missing at T10. **(c)** DSA, right T10 isolated dorsospinal artery injection, PA view. The T10 dorsospinal component missing from the right T10–T11 trunk arises as a separate vessel at the T10 level.

A thoracic vertebral artery is a variant of unilateral intersegmental trunk in which two or more upper thoracic ISAs are joined by anastomoses passing though costotransverse spaces [17]. Descending thoracic vertebral arteries originate from the proximal segment of a normal cervical vertebral artery (Fig. 3.10). Ascending thoracic vertebral arteries arise from the aorta;

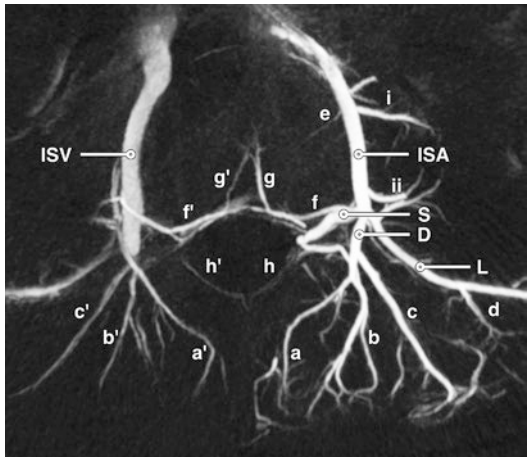

Fig. 3.6 FPCA of the left L2 intersegmental artery in a child, axial reconstruction. The stem of the left L2 ISA (ISA) divides into spinal (S), lateral (L), and dorsal (D) branches. The left dorsal branch (D) provides medial (a), intermediate (b), and lateral (c) muscular rami. Corresponding right-sided branches are opacified via anastomotic channels (a′, b′, c′). A posterior perforator (d) of the left lateral branch (L) is documented; these vessels often contribute to the paravertebral muscular supply. This injection also documents an anterolateral osseous branch (e), bilateral retrocorporeal arteries (f, f′) with their posteromedian osseous branches (g, g′), and bilateral prelaminar arteries (h, h′). Anterolateral muscular branches for the psoas muscle are prominent (i, ii). ISV = right L2 intersegmental vein. (© 2021 Philippe H. Gailloud. All Rights Reserved)

they can—in rare instances—proceed cranially as the ipsilateral cervical vertebral artery and supply the posterior fossa. Thoracic vertebral arteries can be damaged during spine procedures; a widening of the costotransverse space may be the only sign warning of their presence on noninvasive imaging [18].

Traumatic and iatrogenic ISA injuries are best managed by endovascular means [10, 19], but great care must be taken in identifying possible contributions to the spinal cord supply [20] (Fig. 3.11).

The Arterial Supply of the Spinal Cord

Extrinsic Circulation

The spinal cord is vascularized by nine superficial longitudinal anastomotic chains supplied by a small number of anterior and posterior RMAs (Fig. 3.12) [21]. Early during development, each ISA contributes to the cord supply via its spinal branch. The longitudinal chains are made of a succession of anastomoses between these intersegmental contributions (Fig. 3.13) [22, 23].

The primary anastomotic chains, i.e., the anterior and posterolateral spinal arteries, are directly connected to anterior or posterior RMAs. The secondary anastomotic chains, less constant and irregularly distributed, are supplied by lateral branches of the primary chains; they include the anterolateral, lateral, and posteromedian spinal arteries (Fig. 3.14).

A limited number of functionally significant RMAs supplies the adult spinal cord, including the relatively constant anterior vertebrospinal trunks (C1), the superior (C3–C5) and inferior (C7-T1) arteries of the cervical enlargement, the artery of von Haller (T3–T5), and the artery of the lumbosacral enlargement (T6-L4) (Fig. 3.15) [24].

Implication for Spine Intervention

Knowing the location of radicular arteries within the neural foramen is critical for safe needle placement during spine intervention: the superior half of the foramen must be avoided, particularly its anterosuperior quadrant [25] (Fig. 3.16). An artery of Adamkiewicz of low origin or, more often, an accessory vessel such as an *arteria conus medullaris* (L1–L4) [26] or an artery of Desproges-Gotteron (L5-S2) [27] can be injured during spine manipulations [28] or interventions [29]; the resulting spinal cord damage is variable but often limited to the tip of the *conus medullaris*.

Intrinsic Circulation

The intrinsic spinal cord circulation, described by Duret in 1873 [30], includes the sulcal artery and its branches and the perforating rami stemming from the posterior spinal arteries and the *vasocorona* (Fig. 3.17, right hemicord). The sulcal artery takes the name of sulcocommissural artery after penetrating the anterior white commissure at the bottom of the anteriomedian fissure. The territory

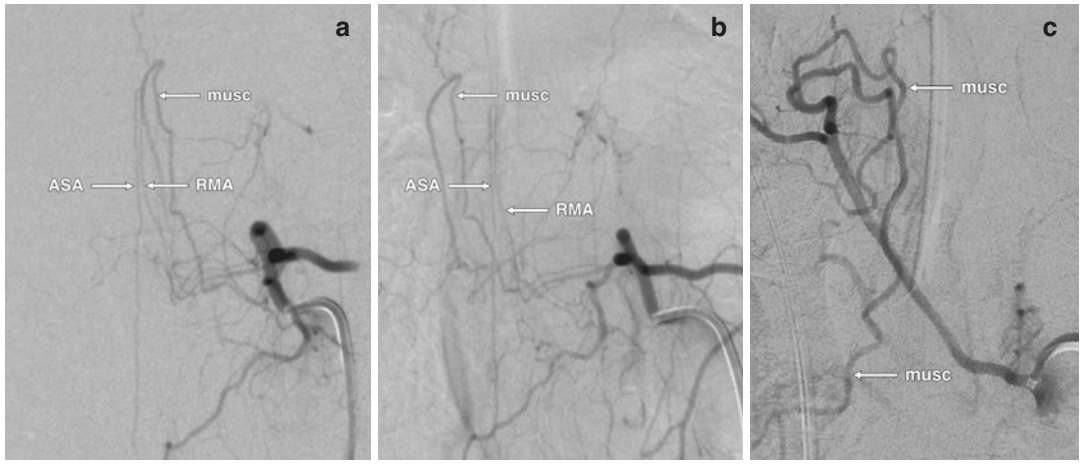

Fig. 3.7 Muscular branches mimicking other vessels. (**a**) Digital subtraction angiography (DSA), left T8 injection, PA projection. This injection documents both an anterior radiculomedullary artery (RMA) supplying the anterior spinal artery (ASA) and a dorsal muscular ramus (musc). The latter may occasionally be confused with an RMA or with the draining vein of a low-flow arteriovenous fistula. In case of doubt, an oblique projection usually helps distinguish muscular branches from other vessels. (**b**) DSA, same as A, oblique projection. The RMA, the ASA, and the muscular branches are easily distinguished in an oblique projection. (**c**) DSA, right T3 injection, postero-anterior projection, showing two prominent muscular branches (musc) mimicking bronchial arteries. (© 2021 Philippe H. Gailloud. All Rights Reserved)

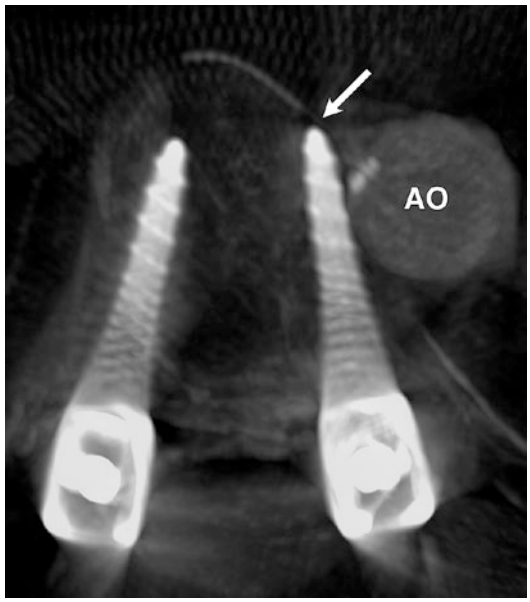

Fig. 3.8 ISA stem compression by an extravertebral pedicular screw. FPCA acquisition during flush aortography prior to revision surgery. This axial image at the T8 level shows the extravertebral location of the tip of the left pedicular screw. The proximal left T8 ISA is narrowed and splayed anteriorly (*arrow*). Besides hemorrhage, ISA stem compression can lead to spinal cord ischemia when the involved vessel provides a radiculomedullary artery. In this case, the artery of Adamkiewicz arose from right T10, and the vascular conflict had no consequence. (© 2021 Philippe H. Gailloud. All Rights Reserved)

of most sulcal arteries is unilateral [31, 32]: the injury of a single sulcal artery can thus lead to a limited unilateral lesion of the anterior gray matter (sulcal syndrome).

Adamkiewicz understood the hemodynamic significance of the division of the intrinsic arteries in central and peripheral territories and introduced the notion of centrifugal and centripetal circulations [33]. While the two circulations communicate at the capillary level, this anatomical continuity has no collateral supply potential: the intrinsic arteries are—from a functional standpoint—terminal arteries [26]. As a result, the interface between the centrifugal and centripetal circulations constitutes a watershed area. When combined with the gray matter's increased sensitivity to ischemia, this watershed area accounts for isolated lesions of the anterior or posterior horns observed during the earliest phase of spinal ischemia and described under the name of "snake-eye" or "owl-eye" lesions (Fig. 3.17, left hemicord).

Implications for Spine Intervention

Spinal ischemia complicating endovascular or percutaneous procedures overwhelmingly concerns the anterior circulation. This is in large

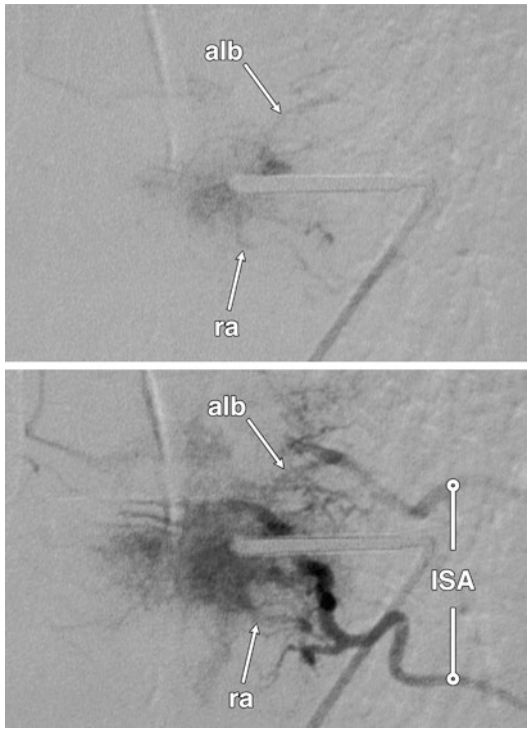

Fig. 3.9 Vertebral phlebography during vertebral body biopsy. Brisk arterial backflow was noted during an otherwise unremarkable T10 vertebral biopsy in a context of pathological fracture. Phlebography through the outer biopsy needle, performed to evaluate the source of the backflow, documented a dense tumoral blush with rapid passage of the contrast agent into two right-sided thoracic intersegmental arteries (ISA), notably via a retrocorporeal artery (ra) at T10 and a network of anterolateral osseous branches (alb) at T9. A small radiculomedullary artery hiding behind the blush would be hard to detect in that example. The backflow was controlled by the insertion of a few Gelfoam® pledgets. The histopathological diagnosis was metastatic adenocarcinoma of unknown origin. This observation shows that retrograde arterial progression of material percutaneously injected into a vertebral body, a risk well recognized with vascular tumors and malformations, may even exist with hypervascular metastatic lesions. (© 2021 Philippe H. Gailloud. All Rights Reserved)

measure due to the more plexiform and redundant configuration of the posterior circulation, which includes four interconnected longitudinal chains supplied by a larger number of afferent RMAs. The classic anterior spinal artery syndrome described in 1908 as an infarct involving the anterior two-thirds of the cord [34] is rarely observed in practice. Instead, gray matter lesions, often restricted to the anterior horns, are common, notably in a context of subocclusive or repeated arterial injury (*Illustrative case 3*). Posterior spinal infarcts may be uni- or bilateral and, contrary to a common misconception, can also lead to profound motor weakness.

A higher number of functional anterior RMAs and more robust paravertebral collateral pathways afford young children some protection against spinal arterial injuries, a capacity that rapidly decreases with age. The anterior circulation of older adults often relies on a single RMA, which cannot be injured without dramatic consequences. The rules established by Lazorthes in 1971 remain valid [26]:

(i) "the nearer the arterial obstruction is to the aortal origin and the farther it is removed from the spinal cord, the greater the possibilities of anastomotic substitution."
(ii) "the slower the obstruction is in establishing itself, the greater the chances of effective intervention by the substitution pathways, whereas a sudden obstruction takes the substitution pathways by surprise."

The Osseous Vascularization

The vertebral body is supplied by anterolateral and posterior osseous branches (Fig. 3.18). Anterolateral branches arise from the ISA stem and penetrate the periphery of the vertebral body. Posteromedian branches, derived from the retrocorporeal artery, pass through the basivertebral foramen. Superficial and deep branches of both groups can act as collateral pathways. The posterior elements are supplied by the dorsal branch of the ISA and by the prelaminar artery. Readers interested in a detailed account of the spinal osseous vascularization are referred to Crock [8, 35] and Ratcliffe [36, 37].

Anterolateral Osseous Arteries

Anterolateral osseous arteries are divided into two groups [8]:

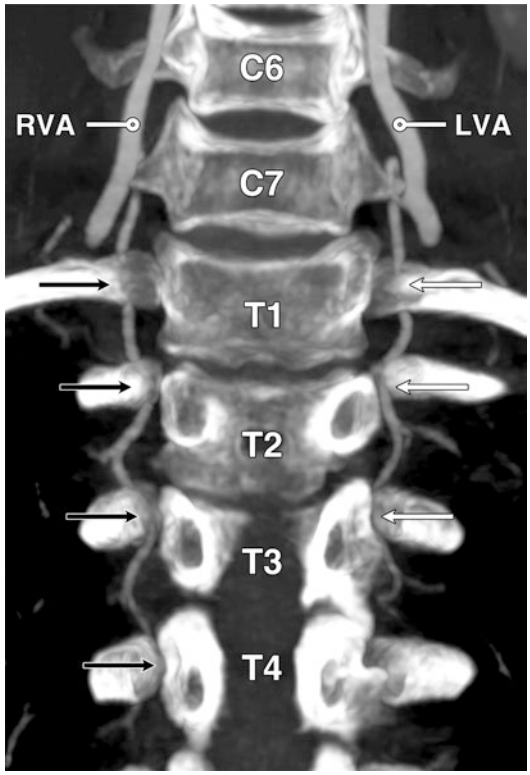

Fig. 3.10 Bilateral thoracic vertebral arteries (VA). The left and right VAs (LVA and RVA) have a normal takeoff from the ipsilateral subclavian artery and enter the transverse canal at C6. Each VA branches off a descending thoracic VA that curves down and enters the C7 transverse foramen before crossing the T1, T2, T3, and T4 costotransverse spaces on the right (*black arrows*) and the T1, T2, T3 costotransverse spaces on the left (*white arrows*).

Fig. 3.11 Radiculomedullary contributions during intersegmental artery embolotherapy. Left T3 angiogram obtained during embolotherapy for hemoptysis post-thoracic surgery. This injection documents both an anterior radiculomedullary artery (*short white arrow*) supplying the anterior spinal artery (*long white arrow*) and a posterior radiculomedullary artery (*short black arrow*) supplying the left posterior spinal artery (*long black arrow*). During endovascular procedures, it is critical to keep in mind the possible presence of branches supplying the spinal cord, which—as shown by this example—frequently lie at the periphery of the field of view and are partially obscured by subtraction and motion artifacts. (Courtesy of Kelvin K. Hong, MBBCh, MBBS, Interventional Radiology, The Johns Hopkins University, Baltimore MD)

(i) Centrum branches that penetrate the vertebra via small foramina located beneath the ISA; most centrum branches are short with only one or two longer *anterolateral equatorial arteries* reaching the central part of the vertebra.
(ii) Ascending, descending, and recurrent branches coursing over the anterolateral surface of the vertebra (Fig. 3.19).

Right thoracic ISA stems, being longer because of the leftward position of the aorta, provide more anterolateral osseous branches [9]. The recurrent branch has a short ascending course before it curves medially to join its counterpart across the midline [9]. The ascending and descending branches either penetrate the vertebra near the endplates or continue across the intervertebral disc space to form an anterolateral network with similar branches from adjacent levels. Ratcliffe counted between 10 and 20 ascending and descending branches at the lumbar level [36]. The most lateral longitudinal connection is the precostal or pretransverse anastomosis; it is typically more robust at L4 to take part in the supply of the L5 vertebra but can be involved in the formation of unilateral intersegmental trunks at any level.

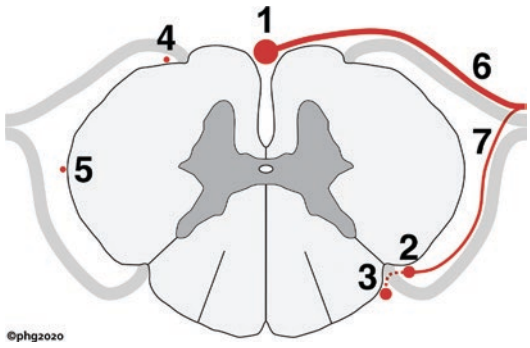

Fig. 3.12 The extrinsic spinal cord circulation. The spinal cord is supplied by primary and secondary longitudinal spinal chains. The primary chains include the anterior spinal artery (1) and the posterolateral spinal arteries (2), which are directly connected to anterior (6) and posterior (7) radiculomedullary arteries. The secondary longitudinal chains are the posteromedial (3), anterior-lateral (4), and lateral (5) spinal arteries. At the cervical level, where both the posteromedial and posterolateral spinal arteries may be prominent, the latter is sometimes called the "lateral spinal artery of the upper cervical spinal cord" [21]. In between the longitudinal chains, the spinal cord is covered by a loose superficial arterial mesh, the *vasocorona.*

Two horizontal anastomotic vessels link the vertical periosteal branches in the metaphyseal regions, more prominently cranially than caudally (Ratcliffe's metaphyseal anastomoses [36]). The intraosseous arteries vascularizing the metaphyseal zones (i.e., the metaphyseal arteries) arise either from the ascending and descending anterolateral branches or from their metaphyseal anastomoses [36].

Anterolateral branches can vascularize posteriorly located vertebral lesions, hypervascular tumors notably, via intraosseous anastomoses. The notion that ISAs exclusively provide anterolateral branches to their matching vertebral body is incorrect, notably in the upper thoracic region, where elongated aortic stems can supply multiple vertebrae via *en passant* branches.

Posteromedian Osseous Arteries

Four retrocorporeal branches converge toward each basivertebral foramen, two ascending branches from the corresponding ISA and two descending branches from the level above (Fig. 3.20a) [38]. From their point of connection arise one or two large nutrient arteries that pass through the basivertebral foramen or, less often, a small accessory canal [36, 39] (see Fig. 3.6). Retrocorporeal arteries are prominent in children, in whom the posteromedian osseous circulation prevails; descending branches tend to disappear with age (Fig. 3.20b, c).

Embolization of vascular malformations or tumors often involves retrocorporeal arteries, which are frequently connected to a radiculomedullary branch (Fig. 3.21). The blush associated with the cluster of posteromedian branches converging toward the basivertebral foramen may mimic a pathology (Fig. 3.22). A normal vertebral blush can also be difficult to distinguish, on a single angiographic projection, from a benign condition (e.g., an enhancing Schmorl node) or an aggressive lesion (e.g., an osseous or lymph node metastasis). In such instances, an oblique projection (Fig. 3.23) or a three-dimensional acquisition may be necessary (Fig. 3.24).

A small group of posterolateral arteries originating from the spinal branch of the ISA can occasionally provide an atypical supply to vertebral lesions.

Vascularization of the Posterior Arch

The posterior elements of the vertebra are supplied by the prelaminar artery, which lies on the inner surface of the lamina, and by the dorsal branch of the ISA, which courses along the outer surface of the lamina and spinous process (see Figs. 3.6 and 3.18). The dorsal branch provides multiple rami to the lamina, the posterior vertebral joint, and the spinous process; ascending and descending muscular branches form a complex paravertebral arterial network [8].

Sometimes described as a branch of the radicular artery, the prelaminar artery is more often a distinct vessel arising from the dorsal division of the ISA (Figs. 3.18 and 3.25). Prelaminar arteries from adjacent levels form a network over the anterior aspect of the posterior arch comparable to the retrocorporeal network covering the posterior vertebral wall. Although the prelaminar mesh features smaller and "more closely woven" arter-

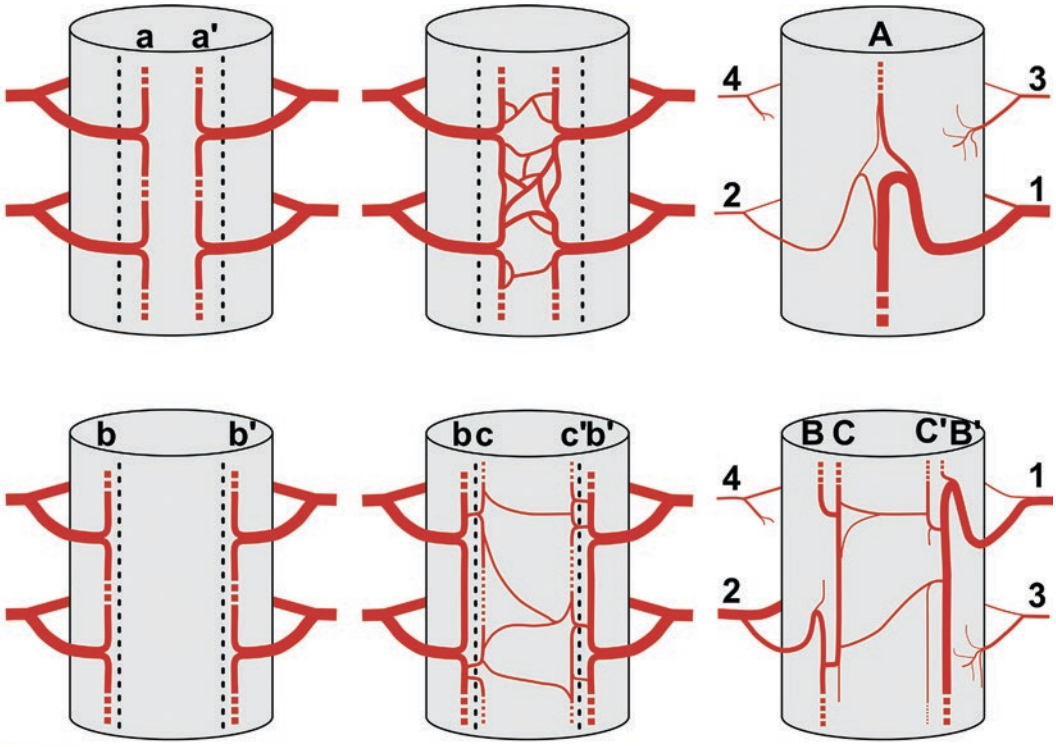

Fig. 3.13 Development of the anterior (top) and posterior (bottom) spinal arteries. *Top left*: Initially, a ventral extension of each spinal branch reaches the neural tube and provides ascending and descending rami that establish anastomoses with adjoining vessels. These anastomotic chains form the primitive anterolateral spinal arteries (a and a′). *Top center*: Each primitive anterolateral spinal artery participates in the formation of a dense midline network, from which will emerge a single median vessel, the anterior spinal artery (ASA). The mechanism behind this process is not fully elucidated but may involve the fusion of primitive vascular segments, the selection of an optimal path within the mesh, or both. *Top right*: At the adult stage, the ASA (A) is supplied by a limited number of prominent radiculomedullary arteries (1). Smaller, possibly subangiographic branches lacking a significant functional role under normal circumstances may remain connected to the longitudinal chain (2). Branches ending over the surface of the cord (3) or at the root level (4) have been named radiculopial and radicular arteries, respectively [22]. This mode of development explains the relatively common observation of ASA duplications. *Bottom left*: Dorsal extensions of each intersegmental spinal branch also reach the neural tube. However, because they course over the anterior aspect of the posterior nerve rootlets, their ascending and descending rami form longitudinal anastomotic chains—the primitive posterolateral spinal arteries (b and b′)—in front of the dorsal root entry zone (*dotted lines*). *Bottom center*: The formation of a single midline mesh is likely impaired by the lateral position of the primitive posterior spinal arteries, ventral to the dorsal root entry zone; instead, the primitive chains send small rami through the nerve rootlets to form a second pair of anastomotic chains along their medial aspect, the primitive posteromedial spinal arteries (c and c′), which loosely interconnect across the midline. *Bottom right*: At the adult stage, two pairs of posterior longitudinal chains are identified, the posterolateral (B and B′) and posteromedial (C and C′) spinal arteries. They have an irregular mesh-like appearance (i.e., Gillilan's posterior spinal network [23]). Posterior radiculomedullary arteries (1, 2) are slightly more common than anterior ones; posterior branches can also terminate within the pial surface (radiculopial, 3) or the along the nerve root (radicular, 4).

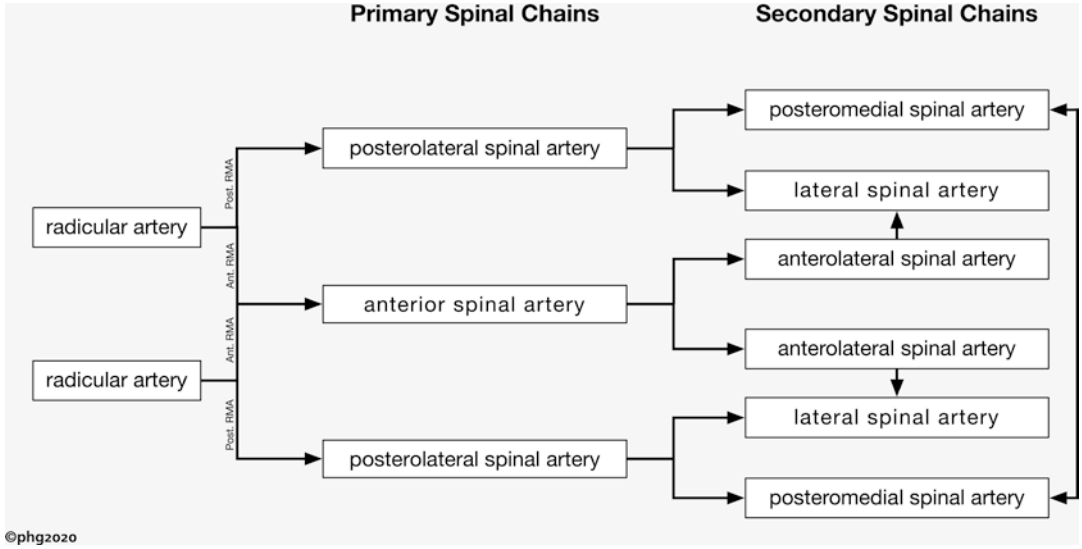

Fig. 3.14 Primary and secondary longitudinal anastomotic chains. Radicular arteries provide anterior and posterior radiculomedullary branches (Ant. and Post. RMA), which form the primary longitudinal chains. The secondary longitudinal chains are supplied indirectly via the primary chains. (© 2021 Philippe H. Gailloud. All Rights Reserved)

ies [8], the two networks can be difficult to differentiate angiographically. The proximal prelaminar artery sends a branch into the base of the lamina, which bifurcates into ascending and descending rami for the apophyseal joints. The distal prelaminar artery ends into an anastomosis with its contralateral counterpart, from which arises a central artery that penetrates the base of the spinous process. Additional medial twigs vascularize the epidural fat and the thecal sac and can participate to the supply of posteriorly located spinal arteriovenous malformations. The posterior elements, less robustly supplied than the vertebral body, are more prone to ischemia during surgical procedures [8].

Intraosseous Arterial Architecture

The arterial architecture of the vertebral body may be divided into central and peripheral components. The central component is vascularized by an "arterial grid" principally supplied by posteromedian branches and reinforced by a few robust anterolateral equatorial arteries (see Fig. 3.18) [8]. The central grid sends ascending and descending rami to the corresponding portion of the endplates.

The peripheral component is vascularized by a superficial network that depends anteriorly on the ISA stem and posteriorly on the retrocorporeal artery. Intraosseous arteries penetrate the vertebra circumferentially and send vertical rami to the portion of the endplates not supplied by the central grid.

The Vertebral Blush and Its Evolution with Age

Selective ISA angiography normally results in a dense capillary blush limited to the ipsilateral half of the vertebral body, i.e., the hemivertebral blush. The extent and conspicuity of this blush depend on connections established between the anterolateral and posteromedian osseous arteries (intraosseous anastomoses) and between adjacent and opposite ISAs (extraosseous anastomoses). This variability can render the identification of a pathological blush challenging.

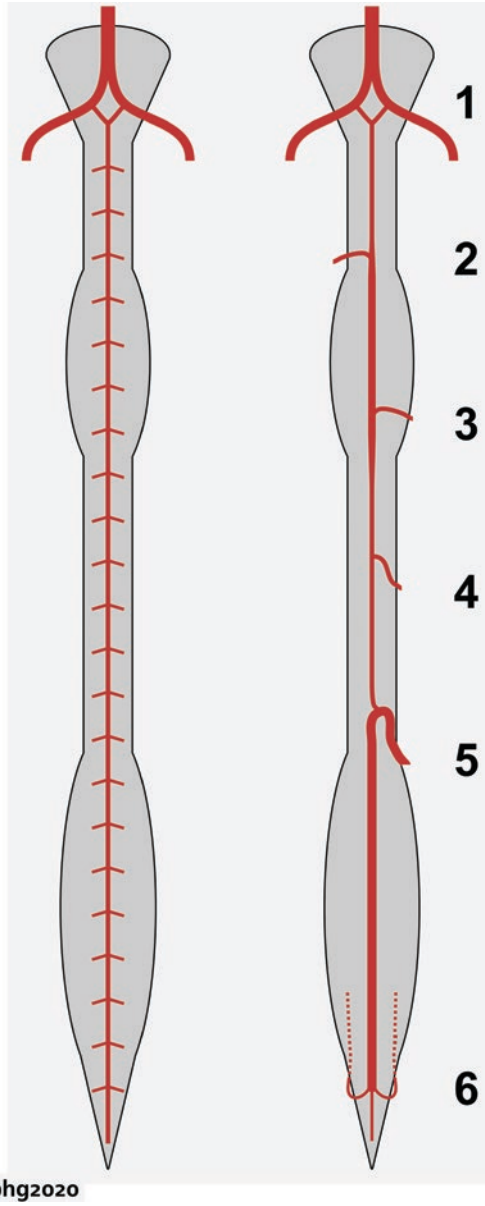

Fig. 3.15 The radiculomedullary arteries. *Left*: The anterior spinal artery is an anastomotic chain rather than a true vessel. It initially receives intersegmental contributions at each vertebral level. *Right*: The arterial supply later adapts to the increased metabolic demand of the gray matter masses in the cervical and lumbosacral regions. Only a few constant and functionally important afferent vessels remain, including the anterior vertebrospinal trunks (1), the superior (2) and inferior (3) arteries of the cervical enlargement, the artery of von Haller (4), and the artery of the lumbosacral enlargement (5). The periconal arterial anastomotic circle (6), which is equivalent to the circle of Willis at the cerebral level, is under normal circumstances the only functional connection between the anterior and posterior spinal circulations [24]. (© 2021 Philippe H. Gailloud. All Rights Reserved)

In newborn and infants, the main supply comes from posteromedian osseous branches. Only one or two anterolateral branches are initially present, their size and number increasing with age [36]. This dominance shift results in a progressive transition from a central blush in children to a hemivertebral blush in adults. Another feature of the blush in children is the existence of a linear contrast uptake along the upper and lower endplates, which slowly fades before disappearing, at about age 20, with the closure of the vertebral growth plates. The conversion of the rich intravertebral arterial network seen in children to the functional end-artery configuration of adults—completed by age 15—also plays a role [37]. Finally, the replacement of the vertebral bone marrow by fat tissue during life's later stages weakens the blush in older patients. Four age-related vertebral blush patterns may thus be distinguished (Fig. 3.26):

(i) *Type I*—Dominant linear endplate blush, minor or absent central vertebral body blush
(ii) *Type II*—Concomitant endplate and central vertebral body blushes
(iii) *Type III*—Hemivertebral blush without linear endplate blush (typical adult appearance)
(iv) *Type IV*—No detectable blush despite a technically adequate injection

Implications for Spine Intervention

Any osseous or periosteal artery can participate in the formation of anatomic variants (e.g., unilateral trunks) or collateral pathways. Connections may involve homologous branches (e.g., left and right recurrent arteries), heterologous vessels (e.g., anterolateral to posteromedian osseous arteries), or even visceral branches (Fig. 3.27). Being aware of these pathways and their potential connections with functionally important branches is critical during endovascular procedures.

The vertebral body vascularization intermingles arteries, capillaries, and veins in a constricted space. This angioarchitecture favors the passage of embolic material from one vascular compartment to another, for example, during ver-

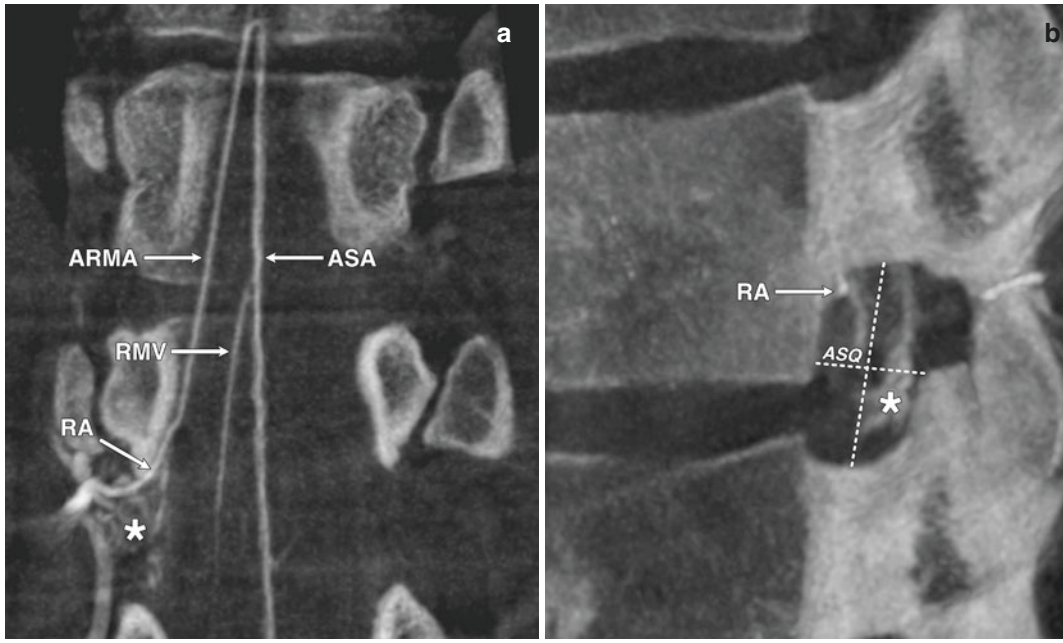

Fig. 3.16 Location of thoracolumbar radicular arteries within the neural foramen documented by flat panel catheter angiotomography (FPCA). (**a**) FPCA, right T12 injection, coronal reconstruction. A right T12 radicular artery (RA) continues as an anterior radiculomedullary artery (ARMA) supplying the anterior spinal artery (ASA). This reconstruction also documents an anterior radiculomedullary vein (RMV) and the epidural plexus at T12-L1 (*asterisk*). (**b**) FPCA, right T12 injection, sagittal reconstruction. The radicular artery (RA) passes immediately under the T12 pedicle, crossing the anterosuperior quadrant (ASQ) of the neural foramen. Epidural venous structures (*asterisk*) are seen in superprojection. A recent study found 96.2% of radicular arteries within the anterosuperior quadrant and none within the posteroinferior quadrant [25]. (© 2021 Philippe H. Gailloud. All Rights Reserved)

tebral augmentation procedures but also in the setting of fibrocartilaginous embolic stroke. Trauma or the placement of intervertebral foreign bodies such as needles can lead to the development of intraosseous arteriovenous fistulas (*Illustrative case 4*).

Brief Case Illustrations

Case 1: Lumbar Pseudoaneurysm After Trauma and Surgery

Patient with multiple traumatic injuries including a burst fracture of L5. A CT obtained 3 weeks after the initial trauma showed a pseudoaneurysm adjacent to the fractured vertebra, which was not present on prior imaging studies, including a CT performed immediately after surgical stabilization two and a half weeks earlier (Fig. 3.28). This pseudoaneurysm, likely caused by secondary displacement of a bone fragment, highlights the risk of delayed vascular injuries.

Case 2: Spinal Cord Ischemia After Vertebral Augmentation

Paraparesis after microwave ablation and vertebral augmentation of a T7 metastatic lesion in a patient with breast cancer. Postprocedural MRI documented acute spinal cord ischemia (Fig. 3.29a). Angiography with flat panel catheter angiotomography (FPCA) obtained 5 days later showed mass effect caused by extravertebral bone cement on the left T7 ISA, which provided a prominent anterior RMA, and occlusion of the anterior spinal artery (Fig. 3.29b, c, d).

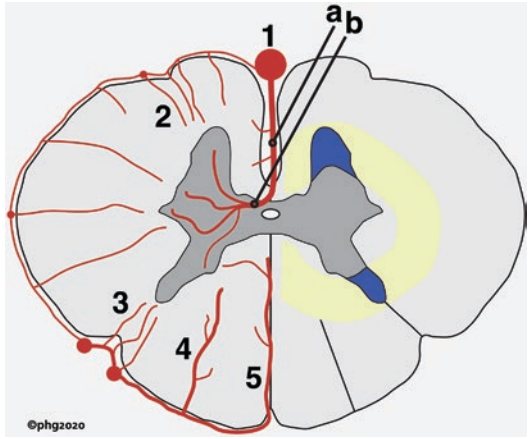

Fig. 3.17 The intrinsic spinal cord circulation. *Right hemicord*—The scheme follows Duret's original description [30]. Sulcal arteries (a) are dorsal branches of the anterior spinal artery (1); they take the name of sulcocommissural arteries (b) deep in the anteromedian fissure as they penetrate the cord substance. Sulcal arteries generally have a unilateral distribution, but they can also bifurcate into two or more sulcocommissural branches and provide bilateral supply [31]. The scheme also shows the anterior (2) and posterior (3) radicular arteries of Duret, the artery of the intermediate fissure (4), and the artery of the posteromedian fissure (5). *Left hemicord*—a circular watershed area (yellow) lies at the interface between the central and peripheral arterial circulations. The portions of gray matter located within that watershed area are at the highest risk of ischemia, explaining the typical bilateral dot-like appearance suggestive of owl or snake eyes on axial T2-weighted MRI. (© 2021 Philippe H. Gailloud. All Rights Reserved)

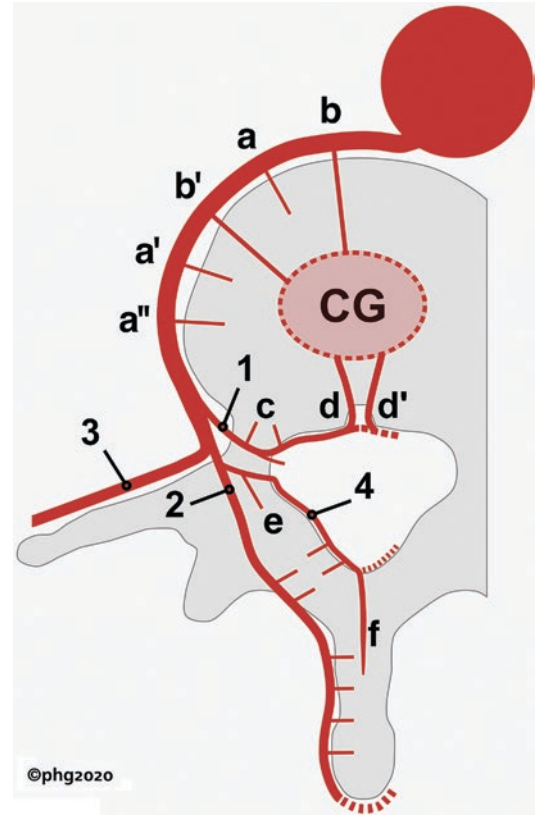

Fig. 3.18 Schematic view of the vertebral vascularization. The intersegmental artery (ISA) divides into spinal (1), dorsal (2), and lateral (3) branches. The prelaminar artery (4) arises from the dorsal branch of the ISA. Centrum branches arise from the ISA stem and enter the vertebral body radially; while most are short (a, a′, a″), one or two longer branches, the anterolateral equatorial arteries (b, b′), participate in the supply of the central grid (CG). The spinal division of the ISA divides into radicular and retrocorporeal arteries. The retrocorporeal artery branches off posterolateral (c) and posteromedian (d, d′) osseous arteries. The latter enter the basivertebral foramen to reach the CG. The posterior elements are vascularized by the dorsal branch of the ISA (2) and by the prelaminar artery (4). The proximal portion of the prelaminar artery sends off a laminar artery (e) into the lamina to supply the superior and inferior apophyseal joints via ascending and descending rami. The prelaminar artery ends with a central artery (f) that enters the base of the spinous process. The dotted extensions of the retrocorporeal artery, prelaminar artery, and dorsal branch of the ISA indicate frequent anastomotic pathways. (© 2021 Philippe H. Gailloud. All Rights Reserved)

This example shows that mass effect without intravascular passage of bone cement may suffice to cause spinal cord flow impairment and ischemia.

Case 3: Spinal Cord Ischemia from Intrathecal Catheter

Patient with progressive lower extremity paresthesia and weakness that started a few weeks after placement of an intrathecal catheter for the management of lingering pain after a car accident. MRI documented hypersignal in the anterior gray matter of the conus medullaris consistent

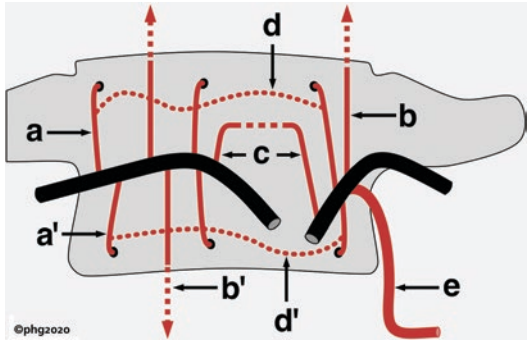

Fig. 3.19 The anterolateral group of osseous branches. The left and longer right ISAs are figured in black; they are cut off at their origin from the aorta. Short ascending (a) and descending (a′) branches end by penetrating the vertebra in the metaphyseal region. Long ascending (b) and descending (b′) branches connect with similar vessels from adjacent levels to form a superficial network. Recurrent branches interconnect across the midline (c). The ascending and descending branches are linked by horizontal anastomotic vessels (d, d′) (Ratcliffe's metaphyseal anastomoses). A robust vertical precostal or pretransverse anastomosis (e) can lead to the formation of a unilateral intersegmental trunk. (© 2021 Philippe H. Gailloud. All Rights Reserved)

with chronic ischemia (Fig. 3.30a). FPCA documented direct contact between the intrathecal catheter and the artery of Adamkiewicz (Fig. 3.30b, c).

Case 4: Intraosseous Arteriovenous Fistula After Vertebral Augmentation

Preoperative embolization of multilevel metastatic disease. A high-flow arteriovenous fistula was noted at T11, level at which percutaneous vertebroplasty had previously been performed (Fig. 3.31a, b). The intraosseous arteriovenous shunt, immediately adjacent to the bone cement mass, was likely created by the tip of the vertebroplasty needle at the time of the procedure (Fig. 3.31c). Traumatic or iatrogenic intraosseous fistulas without intradural drainage in adult patients can remain asymptomatic or cause chronic back or radicular pain syndromes. They can be a source of significant bleeding during surgery.

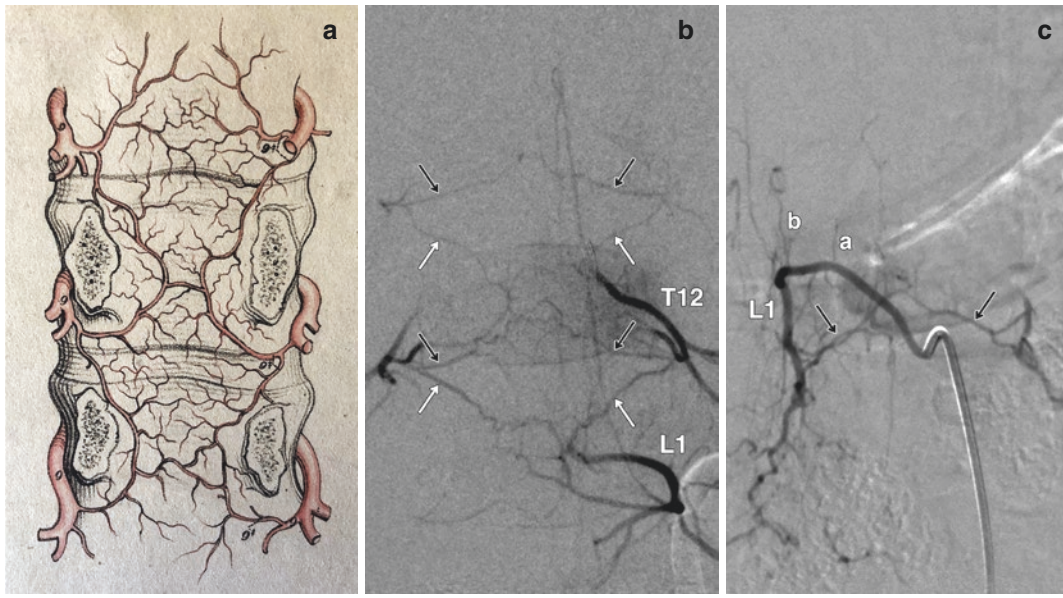

Fig. 3.20 The retrocorporeal network. (**a**) Illustration reproduced from Quain's *The Anatomy Of The Arteries of the Human body* (1844) [38]. Each retrocorporeal artery sends ascending and descending branches that interconnect longitudinally and transversally over the posterior surface of the vertebral body to form a "diamond-shaped" network. The ascending branch provides the posteromedian osseous arteries that enter the basivertebral foramen. The descending branch crosses the subjacent intervertebral space, where it can be compressed by disc bulging. (**b**) Digital subtraction angiography (DSA), left T12 injection in a 3-year-old boy, posteroanterior projection, demonstrating the typical "diamond-shape" pattern of the retrocorporeal network. (*White arrows* = descending branches, *black arrows* = ascending branches). Note a left posterior radiculomedullary artery at L1. (**c**) DSA, right L1 injection in a 58-year-old man, posteroanterior projection. Only the ascending retrocorporeal branches are documented. A progressive loss of the descending branches caused by intervertebral disc bulging is an age-related phenomenon [36]. Short (a) and long (b) ascending anterolateral branches are also documented. (© 2021 Philippe H. Gailloud. All Rights Reserved)

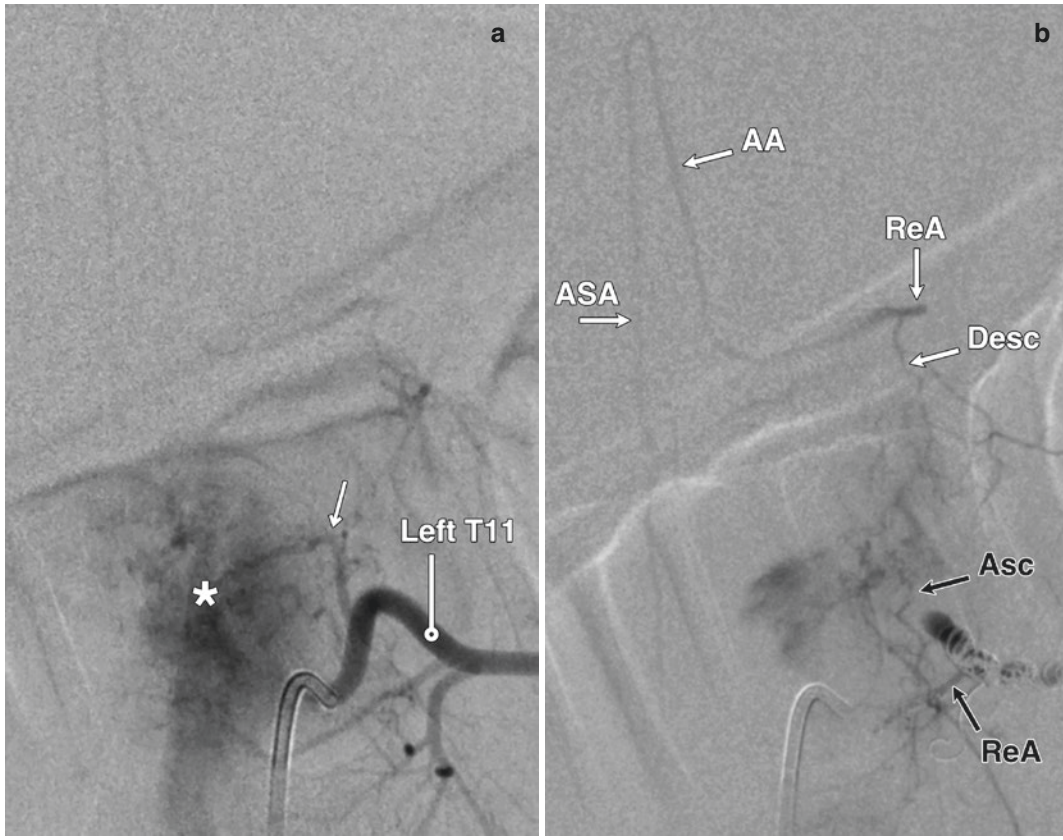

Fig. 3.21 Preoperative embolization of a vertebral metastasis. (**a**) Digital subtraction angiography (DSA), left T11 injection, posteroanterior projection, documenting a tumoral hypervascular blush (*asterisk*). A prominent left T10 anterior radiculomedullary artery, the artery of Adamkiewicz (not labeled in this image), is faintly opacified via collateral pathways. The search for radiculomedullary arteries—identified by their sharp median or paramedian "hairpin-like" curves—must be constant during spinal and paraspinal embolotherapy, including bronchial and mediastinal interventions. Note that the lesion is in part supplied by a robust recurrent anterolateral osseous branch (*arrow*). (**b**) DSA, distal left T11 injection, posteroanterior projection, during embolotherapy. The T11 and T10 retrocorporeal arteries (black and white ReA) are interconnected by their respective ascending (black Asc) and descending (Desc) branches. The artery of Adamkiewicz (AA) and the anterior spinal artery (ASA) are better appreciated. In such circumstance, free-flowing liquid or particulate agents are generally avoided as non-target embolization carries a high risk of spinal cord injury. Hemodynamic alterations occurring during embolization can sometimes expose initially undetectable dangerous anastomoses, highlighting the value of repeated angiograms, notably before the use of liquid embolic agents.

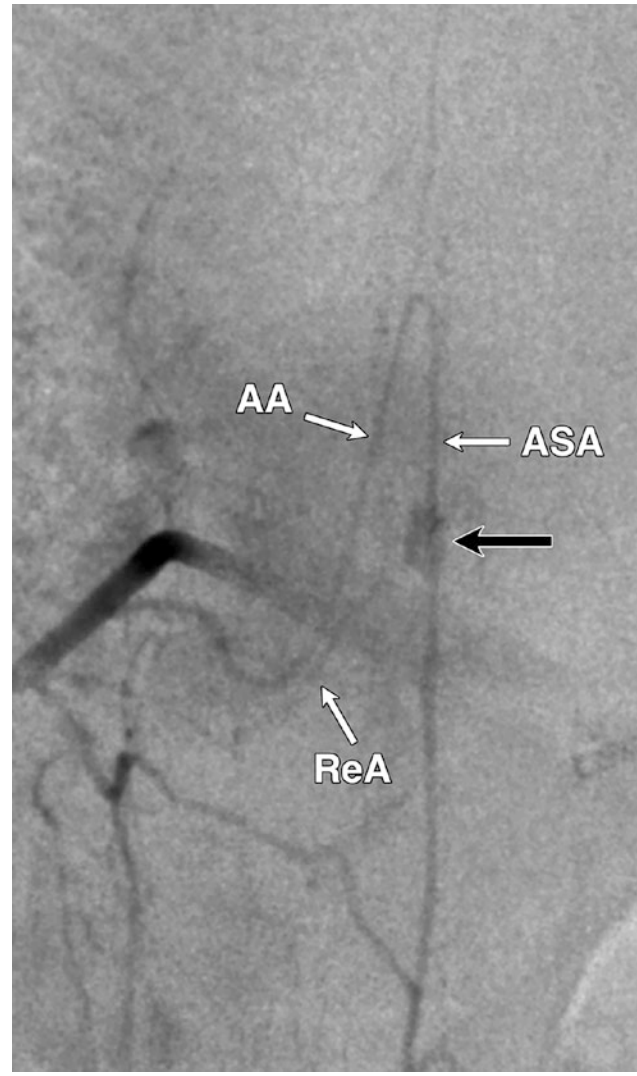

Fig. 3.22 False pathological image. This right T10 injection documents the artery of Adamkiewicz (AA) and the anterior spinal artery (ASA). The blush associated with the posteromedian branches of the retrocorporeal artery (ReA) crowding the basivertebral foramen can mimic a pathology, in this example an aneurysm of the anterior spinal artery (*black arrow*). (© 2021 Philippe H. Gailloud. All Rights Reserved)

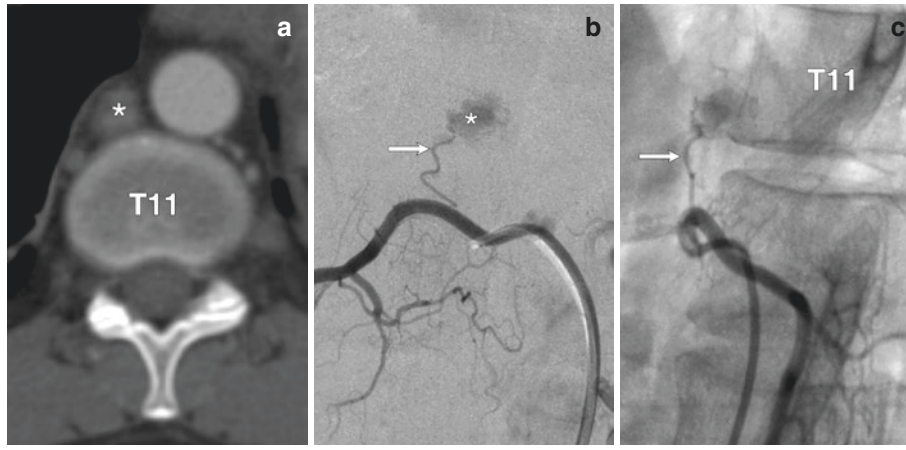

Fig. 3.23 Angiographic appearance of a prevertebral adenopathy. (**a**) CTA, axial image at T11, showing a prevertebral adenopathy (*asterisk*). (**b**) Digital subtraction angiography (DSA), right T12 injection, posteroanterior projection; the blush associated with the adenopathy, supplied by an ascending anterolateral osseous branch (*arrow*), cannot be distinguished from a vertebral lesion in this projection. (**c**) DSA, right T12 injection, oblique projection, clarifying the prevertebral location and nature of the abnormal blush. The *arrow* points at the ascending anterolateral osseous feeder. (© 2021 Philippe H. Gailloud. All Rights Reserved)

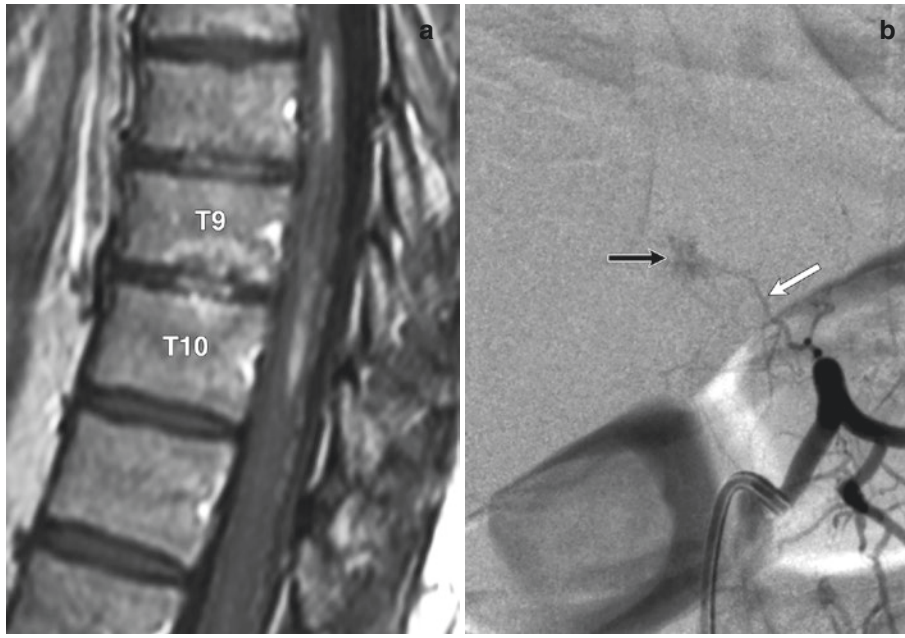

Fig. 3.24 Enhancing Schmorl node in a patient with a spinal cord stroke. (**a**) MRI, sagittal T1 image after gadolinium injection, documenting a heterogeneously enhancing cord anomaly with prominent perimedullary vessels consistent with a subacute infarct with luxury perfusion. Note the enhancing Schmorl node at the T9–T10 intervertebral space. (**b**) Digital subtraction angiography (DSA), left T10 injection, posteroanterior projection, showing a focal blush (*black arrow*) supplied by an anterolateral osseous branch (*white arrow*). (**c**) DSA, left T10 injection, posteroanterior projection, same image with anatomic background. The blush projects over the intervertebral space and can therefore not be related to normal posteromedian osseous branches, as shown in Fig. 3.22. (**d**) Flat panel catheter angiotomography (FPCA), sagittal reconstruction of a left T10 injection. The angiographic blush can be located within the central part of the disc space (circle) and corresponds to the enhancing Schmorl node documented by MRI. (© 2021 Philippe H. Gailloud. All Rights Reserved)

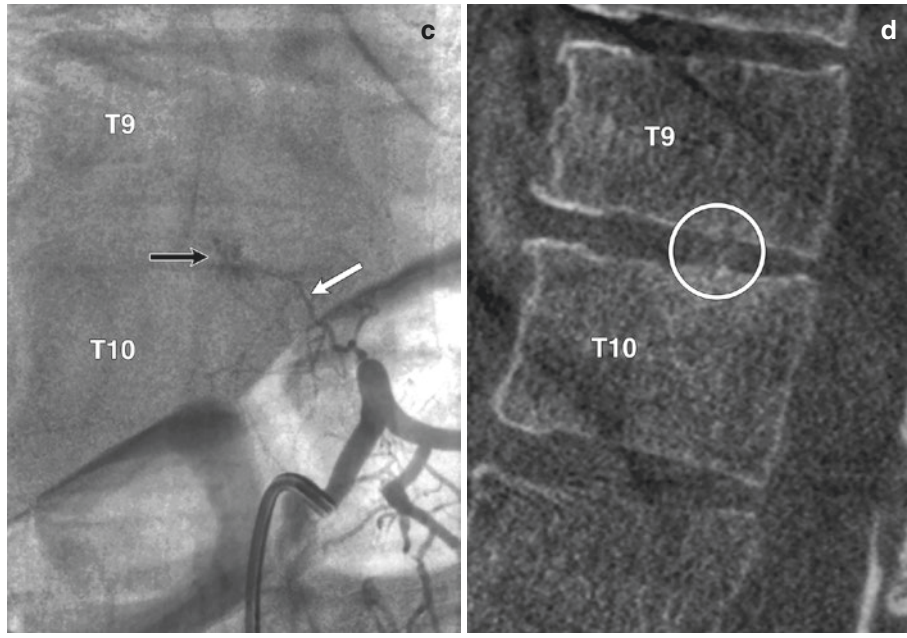

Fig. 3.24 (continued)

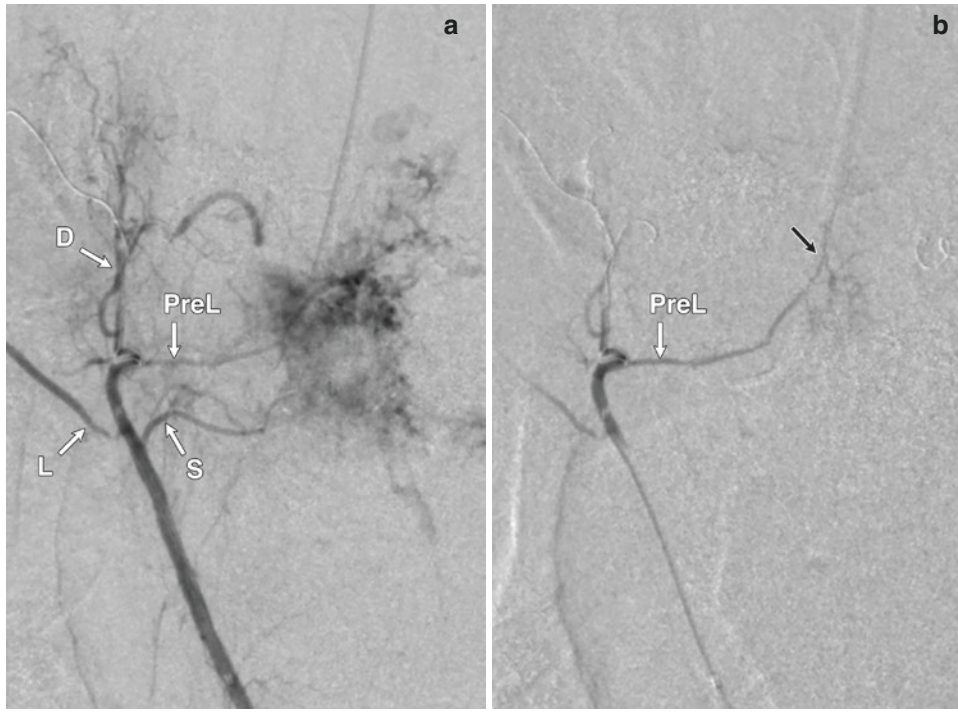

Fig. 3.25 Preoperative embolization of a T4 vertebral metastasis. (**a**) Digital subtraction angiography (DSA), right T4 injection, posteroanterior projection. The ISA divides into spinal (S), lateral (L), and dorsal (D) branches. The spinal division (S) continues as a retrocorporeal artery without radiculomedullary contribution. A robust prelaminar artery (PreL) arises from the dorsal division of the ISA and supplies tumoral tissue in the contralateral lamina. (**b**) DSA, distal right T4 injection, posteroanterior projection. This early arterial phase image documents the anatomy of the prelaminar artery (PreL), including its connection, at the base of the spinous process, with the opposite prelaminar artery via an inversed "V" shaped anastomosis (*black arrow*).

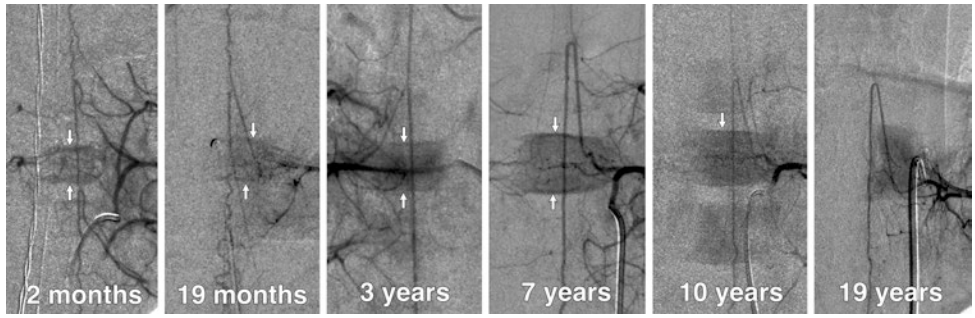

Fig. 3.26 Evolution of the vertebral blush with age. The pace of the vertebral body blush evolution varies between individuals and between vertebrae in the same individual. The anterior spinal artery, opacified in each case, marks the midline. *Type I*—The vertebral body blush initially appears as thick linear enhancement along the endplates (*white arrows*, *2 months*). *Type II*—A focal central blush then becomes detectable (*19 months*); it soon fills to the whole vertebral frame, while the endplate enhancement starts fading (*3 and 7 years*). *Type III*—The endplate blush, barely noticeable at *10 years*, disappears as the vertebral growth plates close near the end of the second decade; the central blush regresses to an adult hemivertebral pattern (*19 years*).

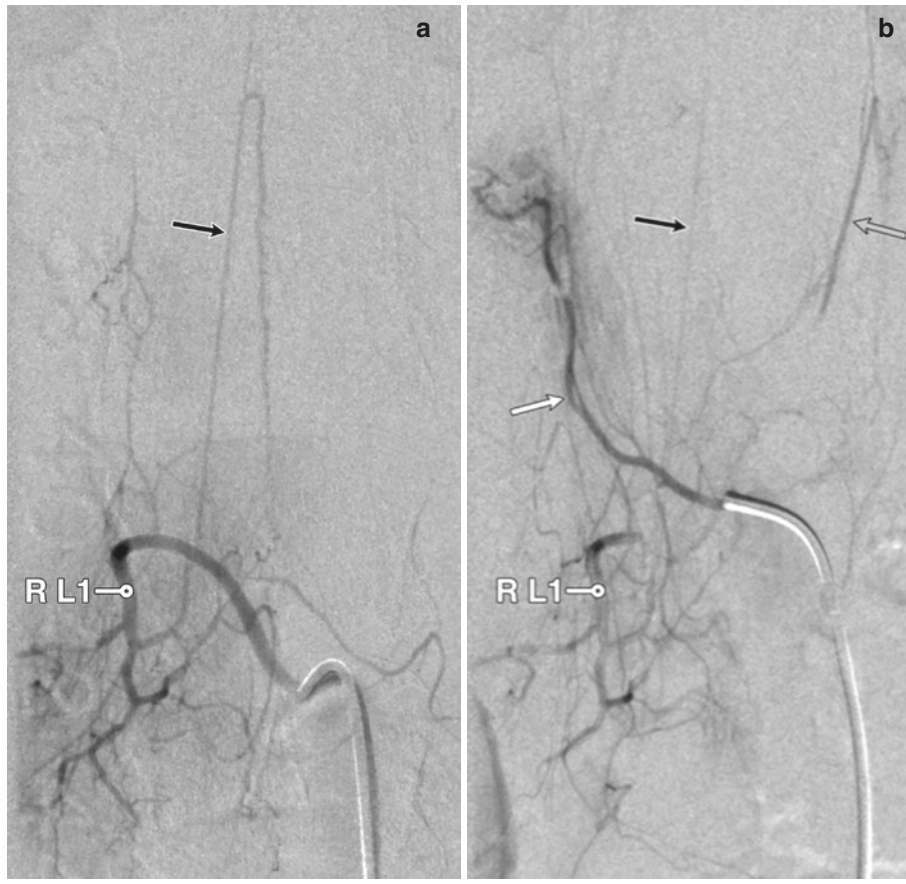

Fig. 3.27 Dangerous anastomoses. (**a**) Digital subtraction angiography (DSA), right L1 ISA injection, posteroanterior projection, documenting the artery of Adamkiewicz (*arrow*). (**b**) DSA, right adrenal artery injection, posteroanterior projection. This selective injection of the right adrenal artery (*white arrow*) also opacifies, via multiple collateral branches, the left adrenal artery (*gray arrow*) and the right L1 ISA and its branches, including the artery of Adamkiewicz (*black arrow*). The artery of Adamkiewicz is faintly opacified and easy to overlook. This example highlights the importance of a detailed investigation of the regional vascular anatomy prior to paravertebral embolotherapy, even when the target is not an ISA.

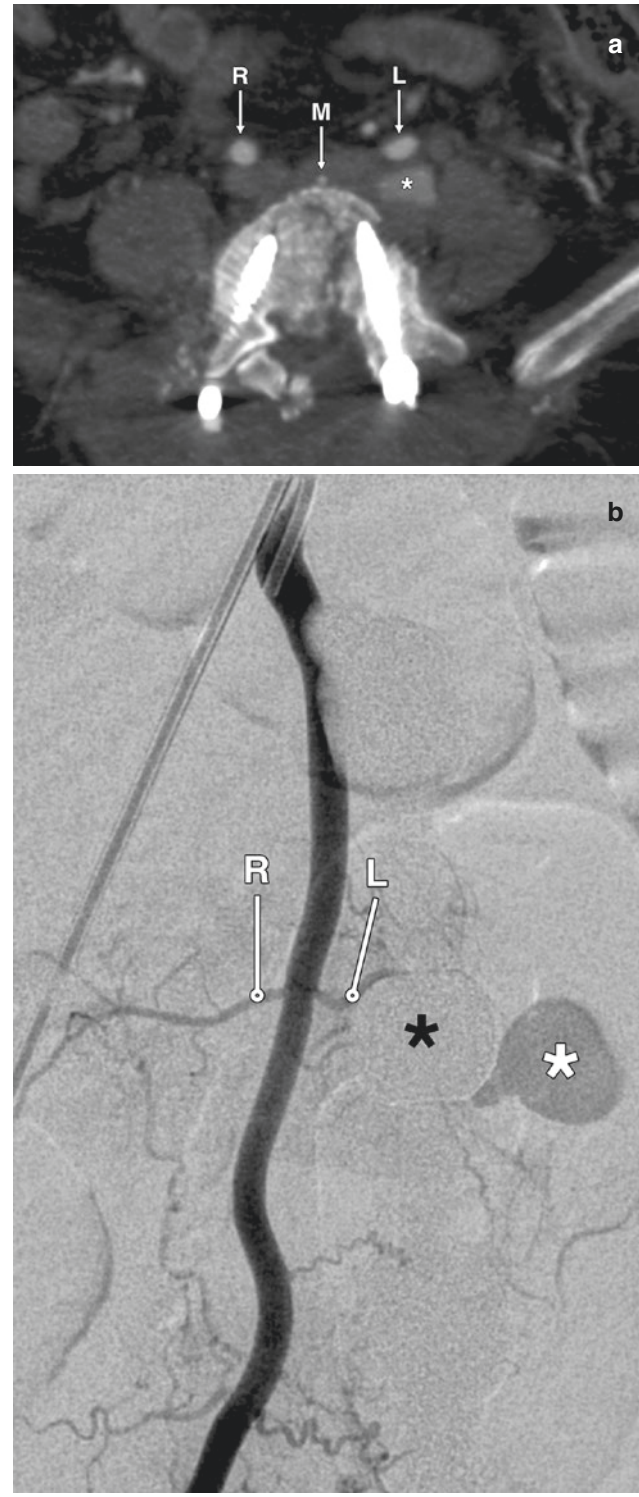

Fig. 3.28 Lumbar pseudoaneurysm after trauma and surgery. (**a**) Contrast-enhanced CT, arterial phase, documenting a pseudoaneurysm (*asterisk*) adjacent to the fractured L5 vertebral body. The letters "L" and "R" indicate the left and right internal iliac arteries. "M" is the median sacral artery. (**b**) Digital subtraction angiography (DSA), median sacral artery injection, posteroanterior projection. The letters "L" and "R" point to the left and right L5 intersegmental arteries (ISA). The pseudoaneurysm (*white asterisk*) is attached to the left L5 ISA (L), which is partially obscured by the subtraction artifact caused by a pedicular screw (*black asterisk*).

Fig. 3.29 Spinal cord ischemia after vertebral augmentation. (**a**) MRI, sagittal diffusion-weighted image, documenting diffusion restriction centered over the T7 level consistent with acute ischemia. (**b**) Digital subtraction angiography (DSA), left T7 injection, posteroanterior projection. The artery of Adamkiewicz (AA) and the anterior spinal artery (ASA) are documented. The descending branch of the ASA is either occluded or partially obscured by subtraction artifacts caused by bone cement. (**c**) Flat panel catheter angiotomography (FPCA), left T7 injection, axial reconstruction. The left T7 ISA (*arrow*), displaced laterally by extravertebral cement (*asterisk*), divides into spinal (a), dorsal (b), and lateral (c) branches. There is no intravascular or intracanalar bone cement. (**d**) FPCA, left T7 injection, oblique reconstruction. The spinal branch of the left T7 ISA provides the AA, which supplies the ASA. The descending branch of the ASA shows an abrupt cutoff (*short white arrow*). The anterior-median spinal vein (ASV) and a left T7 radiculomedullary vein (RMV) are also documented. (Courtesy of Majid Khan, MBBS, MD, Division of Neuroradiology, Head and Neck Imaging, Department of Radiology, Thomas Jefferson University, Philadelphia, Pennsylvania)

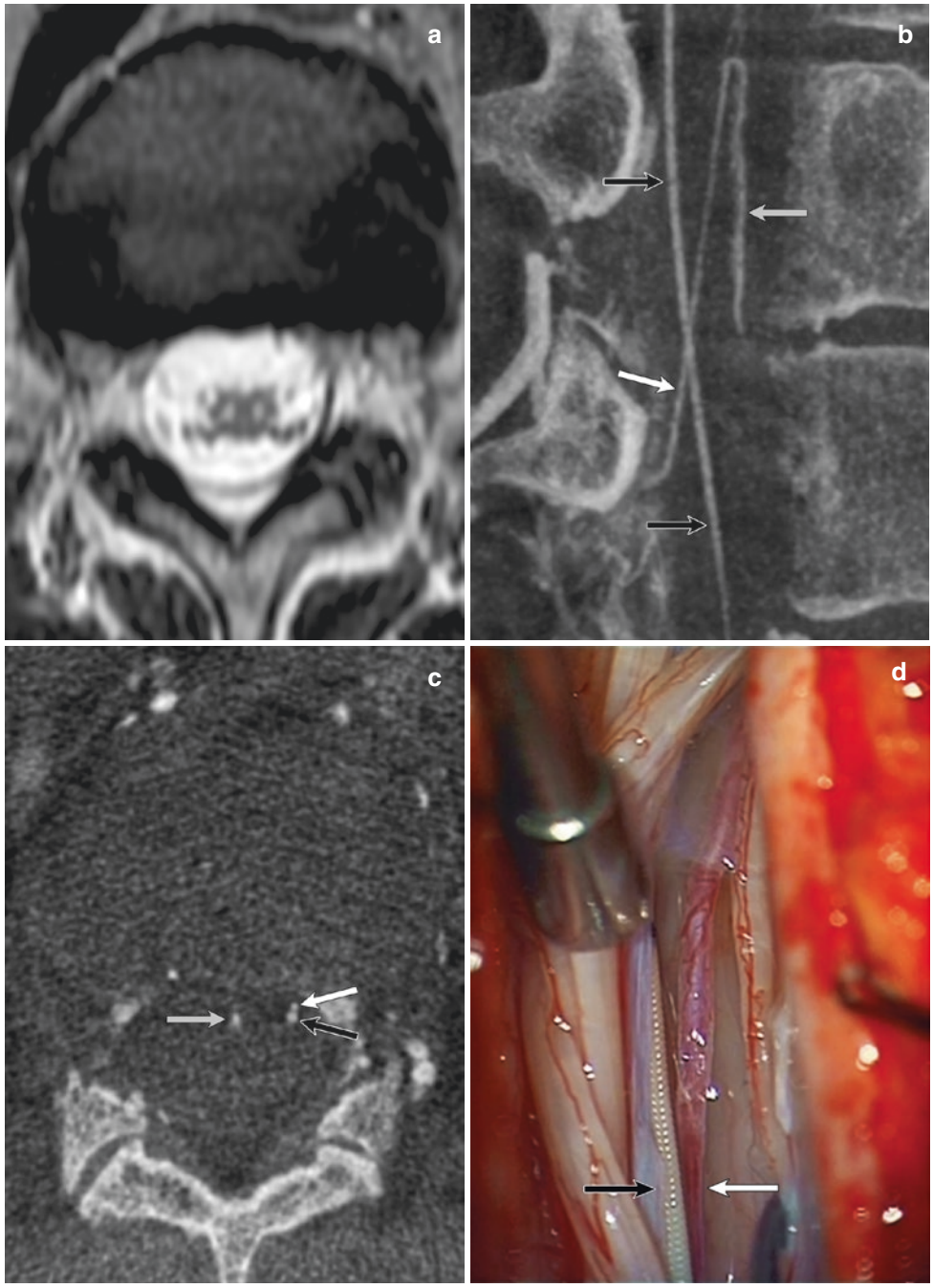

Fig. 3.30 Spinal cord ischemia from intrathecal catheter. (**a**) MRI, axial T2-weighted image, documenting focal bilateral anterior gray matter hypersignal at the conus medullaris level ("snake-eye" appearance), consistent with chronic ischemia. (**b**) Flat panel catheter angiotomography (FPCA), left T12 ISA injection, coronal reconstruction (posterior view). The intrathecal catheter (*black arrows*) crosses the artery of Adamkiewicz (AA) (*white arrow*), which supplies the anterior spinal artery (ASA) (*gray arrow*). (**c**) FPCA, left T12 ISA injection, axial reconstruction, showing the conflict between the AA (*white arrow*) and the intrathecal catheter (*black arrow*). The *gray arrow* points to the ASA ((**a**–**c**) © 2021 Philippe H. Gailloud. All Rights Reserved). (**d**) Operative view (posterior approach) during surgical catheter removal. The portion of the AA (*white arrow*) in conflict with the catheter (*black arrow*), visible after lateral retraction of a nerve root of the cauda equina, appears flattened. ((**d**) Surgical image courtesy of Nicholas Theodore, MD, MS, Department of Neurosurgery, Johns Hopkins University, Baltimore, MD)

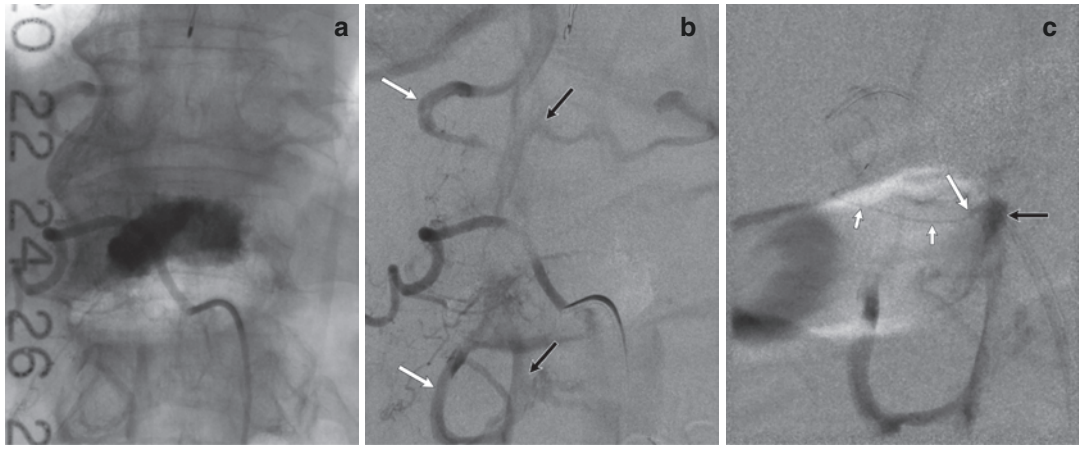

Fig. 3.31 Intraosseous arteriovenous fistula after vertebral augmentation. (**a**) Digital subtraction angiography (DSA), right T11 injection, posteroanterior projection, non-subtracted image showing intravertebral bone cement from a prior percutaneous vertebroplasty. (**b**) DSA, same injection, subtracted image, documenting minor tumoral vertebral blush and immediate widespread opacification of the internal (*black arrows*) and external (*white arrows*) vertebral venous plexuses consistent with a high-flow arteriovenous fistula. (**c**) DSA, injection of a branch of the right T11 retrocorporeal artery, posteroanterior projection. *Short white arrows* outline the position of the microcatheter. This superselective injection confirms the presence of a direct arteriovenous shunt between a feeding artery (*white arrow*) and an intravertebral arterialized venous pouch (*black arrow*), immediately adjacent to the cement mass, without interposition of tumoral blush. ()

References

1. Gailloud P. Multiple thoracic bilateral intersegmental arterial trunks. Eur J Anat. 2017;21(2):149–55.
2. Gailloud P. Vertebral artery triplication. Surg Radiol Anat. 2019;41(7):841–3.
3. Gailloud P. The supreme intercostal artery in its most rudimentary form does not branch off any intercostal arteries. Anat Rec (Hoboken). 2015;298(5):781–2.
4. Gailloud P. The supreme intercostal artery includes the last cervical intersegmental artery (C7) - angiographic validation of the intersegmental nomenclature proposed by Dorcas Padget in 1954. Anat Rec (Hoboken). 2014;297(5):810–8.
5. Chiras J, Merland JJ. The dorsospinal artery. A little known anatomical variant. Its importance in spinal angiography. J Neuroradiol. 1979;6(2):93–100.
6. Siclari F, Fasel JH, Gailloud P. Direct emergence of the dorsospinal artery from the aorta and spinal cord blood supply. Case reports and literature review. Neuroradiology. 2006;48(6):412–4.
7. Doppman JL, Di Chiro G. Paraspinal muscle infarction. A painful complication of lumbar artery embolization associated with pathognomonic radiographic and laboratory findings. Radiology. 1976;119(3):609–13.
8. Crock HV, Yoshizawa H. The blood supply of the lumbar vertebral column. Clin Orthop Relat Res. 1976;115:6–21.
9. Chiras J, Morvan G, Merland JJ. The angiographic appearances of the normal intercostal and lumbar arteries. Analysis and the anatomic correlation of the lateral branches. J Neuroradiol. 1979;6(3):169–96.
10. Santillan A, Patsalides A, Gobin YP. Endovascular embolization of iatrogenic lumbar artery pseudoaneurysm following extreme lateral interbody fusion (XLIF). Vasc Endovasc Surg. 2010;44(7):601–3.
11. Shin HJ, Choi YM, Kim HJ, Lee SJ, Yoon SH, Kim KH. Retroperitoneal hemorrhage from an unrecognized puncture of the lumbar right segmental artery during lumbar chemical sympathectomy: diagnosis and management. J Clin Anesth. 2014;26(8):671–5.
12. Ntourantonis D, Tsekouras V, Korovessis P. Delayed fatal lumbar artery bleeding following less invasive posterolateral decompression and fusion. Spine (Phila Pa 1976). 2018;43(16):E976–9.
13. Biafora SJ, Mardjetko SM, Butler JP, McCarthy PL, Gleason TF. Arterial injury following percutaneous vertebral augmentation: a case report. Spine (Phila Pa 1976). 2006;31(3):E84–7.
14. Tsai YD, Liliang PC, Chen HJ, Lu K, Liang CL, Wang KW. Anterior spinal artery syndrome following vertebroplasty: a case report. Spine (Phila Pa 1976). 2010;35(4):E134–6.
15. Iliopoulos P, Korovessis P, Vitsas V. PMMA embolization to the left dorsal foot artery during percutaneous vertebroplasty for spinal metastases. Eur Spine J. 2014;23(Suppl 2):187–91.

16. Amoretti N, Hovorka I, Marcy PY, Grimaud A, Brunner P, Bruneton JN. Aortic embolism of cement: a rare complication of lumbar percutaneous vertebroplasty. Skelet Radiol. 2007;36(7):685–7.
17. Chiras J, Launay M, Gaston A, Bories J. Thoracic vertebral artery. An anomaly of the vertebral artery. Neuroradiology. 1982;24(1):67–70.
18. Gailloud P, Gregg L, Pearl MS, San MD. Ascending and descending thoracic vertebral arteries. AJNR Am J Neuroradiol. 2017;38(2):327–35.
19. Sclafani SJ, Florence LO, Phillips TF, Scalea TM, Glanz S, Goldstein AS, et al. Lumbar arterial injury: radiologic diagnosis and management. Radiology. 1987;165(3):709–14.
20. Koakutsu T, Aizawa T, Yuzawa H, Itoi E, Kushimoto S. Lumbar artery injury from which the Adamkiewicz artery originated associated with lumbar spine injury: successfully treated by transcatheter arterial embolization. Eur Spine J. 2016;25(Suppl 1):124–8.
21. Lasjaunias P, et al. The lateral spinal artery of the upper cervical spinal cord. Anatomy, normal variations, and angiographic aspects. J Neurosurg. 1985;63(2):235–41.
22. Tanon L. Les artères de la moelle dorso-lombaire. Paris: Vigot Frères, Editeurs; 1908.
23. Gillilan LA. The arterial blood supply of the human spinal cord. J Comp Neurol. 1958;110(1):75–103.
24. Gailloud P, Gregg L, Galan P, Becker D, Pardo C. Periconal arterial anastomotic circle and posterior lumbosacral watershed zone of the spinal cord. J Neurointerv Surg. 2015;7(11):848–53.
25. Gregg L, Sorte DE, Gailloud P. Intraforaminal location of thoracolumbar radicular arteries providing an anterior radiculomedullary artery using flat panel catheter angiotomography. AJNR Am J Neuroradiol. 2017;38(5):1054–60.
26. Lazorthes G, Gouaze A, Zadeh JO, Santini JJ, Lazorthes Y, Burdin P. Arterial vascularization of the spinal cord. Recent studies of the anastomotic substitution pathways. J Neurosurg. 1971;35(3):253–62.
27. Desprogres-Gotteron R. Contribution à l'étude de la sciatique paralysante. Paris: Thèse pour le doctorat en Médecine; 1955.
28. Balblanc JC, Pretot C, Ziegler F. Vascular complication involving the conus medullaris or cauda equina after vertebral manipulation for an L4-L5 disk herniation. Rev Rhum Engl Ed. 1998;65(4):279–82.
29. Wybier M. Transforaminal epidural corticosteroid injections and spinal cord infarction. Joint Bone Spine. 2008;75(5):523–5.
30. Duret H. Note sur les artères nourricières et sur les vaisseaux capillaires de la moelle épinière. Progrès Médical. 1873;1:284.
31. Hassler O. Blood supply to human spinal cord. A microangiographic study. Arch Neurol. 1966;15(3):302–7.
32. Kadyi H. Über die Blutgefässe des Menschlichen Rückenmarkes. Lwów, Poland: Verlag von Gubrynowicz & Schmidt; 1889.
33. Adamkiewicz A. Die Blutgefässe des menschlichen Rückenmarkes. I. Theil. Die Gefässe der Rückenmarkssubstanz. Sitzungsberichten der Kaiserlichen Akademie der Wissenschaften, Mathematisch-naturwissenschaftliche Classe, vol. 84. Wien, Österreich; 1881. p. 469–502.
34. Preobraschenski P. Ein Beitrag zur Lehre von der akuten syphilitischen Poliomyelitis. Neurologisches Centralblatt. 1908;27:1069–74.
35. Crock HV, Yoshizawa H. The blood supply of the vertebral column and spinal cord in man. New York: Springer-Verlag; 1977.
36. Ratcliffe JF. The arterial anatomy of the adult human lumbar vertebral body: a microarteriographic study. J Anat. 1980;131(Pt 1):57–79.
37. Ratcliffe JF. An evaluation of the intra-osseous arterial anastomoses in the human vertebral body at different ages. A microarteriographic study. J Anat. 1982;134(Pt 2):373–82.
38. Quain R. The anatomy of the arteries of the human body, with its applications to pathology and operative surgery. In: Lithographic drawings with practical commentaries. London: Taylor and Walton; 1844. xv, 550 p. and atlas (87 plates in portfolio).
39. Willis TA. Nutrient arteries of the vertebral bodies. J Bone Joint Surg Am. 1949;31A(3):538–40.